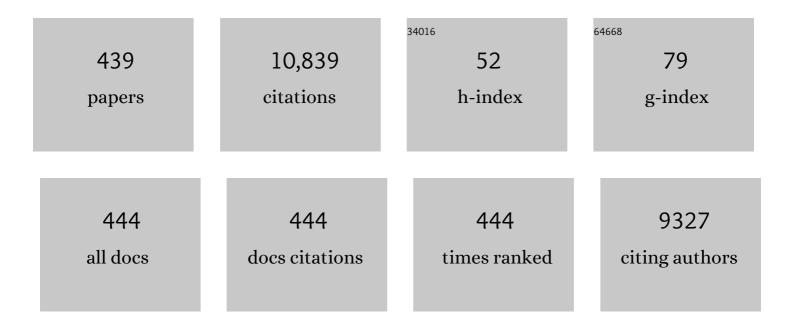
List of Publications by Year in descending order

Source: https://exaly.com/author-pdf/666448/publications.pdf Version: 2024-02-01



#	Article	IF	CITATIONS
1	MoS2/SnO2 heterojunction-based self-powered photodetector. Applied Physics Letters, 2022, 120, . Electrically Modulated Wavelength-Selective Photodetection Enabled by <mml:math< td=""><td>1.5</td><td>9</td></mml:math<>	1.5	9
2	xmlns:mmíl="http://www.w3.org/1998/Math/MathML" display="inline" ´ overflow="scroll"> <mml:msub><mml:mrow><mml:mi>Mo</mml:mi><mml:mi mathvariant="normal">S</mml:mi </mml:mrow><mml:mn>2</mml:mn></mml:msub> <mml:mo>/</mml:mo> < mathvariant="normal">O Heterostructure. Physical Review	mm 1 :5 mmi:mrov	v><11 v> <mml:mi>Z</mml:mi>
3	Applied, 2022, 17, . Infrared photodetectors based on multiwalled carbon nanotubes: Insights into the effect of nitrogen doping. Applied Surface Science, 2021, 538, 148187.	3.1	40
4	Enhanced phase transition and infrared photoresponse characteristics in VO ₂ (M1) thin films synthesized by DC reactive sputtering on different substrates. Materials Advances, 2021, 2, 3726-3735.	2.6	4
5	Solution-Processed SnSe ₂ –RGO-Based Bulk Heterojunction for Self-Powered and Broadband Photodetection. ACS Applied Electronic Materials, 2021, 3, 3131-3138.	2.0	12
6	Electrical transport modulation of VO2/Si(111) heterojunction by engineering interfacial barrier height. Journal of Applied Physics, 2021, 129, .	1.1	7
7	Overcoming the Challenges Associated with the InN/InGaN Heterostructure via a Nanostructuring Approach for Broad Band Photodetection. ACS Applied Electronic Materials, 2021, 3, 4243-4253.	2.0	4
8	Differentiation of ultraviolet/visible photons from near infrared photons by MoS2/GaN/Si-based photodetector. Applied Physics Letters, 2021, 119, .	1.5	19
9	Inhomogeneity-mediated systematic reduction of the Schottky barrier in a Au/GaN nanorod film interface. Semiconductor Science and Technology, 2021, 36, 015017.	1.0	3
10	Defect and strain modulated highly efficient ZnO UV detector: Temperature and low-pressure dependent studies. Applied Surface Science, 2020, 505, 144365.	3.1	46
11	Harvesting energy via stimuliâ€free water/moisture dissociation by mesoporous SnO ₂ –based hydroelectric cell and CuO as a pump for atmospheric moisture. International Journal of Energy Research, 2020, 44, 1276-1283.	2.2	11
12	Temperature-Dependent Electrical Transport and Optoelectronic Properties of SnS ₂ /p-Si Heterojunction. ACS Applied Electronic Materials, 2020, 2, 2155-2163.	2.0	23
13	Temperature Dependent "S-Shaped―Photoluminescence Behavior of InGaN Nanolayers: Optoelectronic Implications in Harsh Environment. ACS Applied Nano Materials, 2020, 3, 8453-8460.	2.4	9
14	Device Architecture for Visible and Near-Infrared Photodetectors Based on Two-Dimensional SnSe2 and MoS2: A Review. Micromachines, 2020, 11, 750.	1.4	19
15	Self-powered, ultrasensitive, room temperature humidity sensors using SnS2 nanofilms. Scientific Reports, 2020, 10, 14611.	1.6	20
16	Defect-Mediated Transport in Self-Powered, Broadband, and Ultrafast Photoresponse of a MoS ₂ /AlN/Si-Based Photodetector. ACS Applied Electronic Materials, 2020, 2, 944-953.	2.0	40
17	Iron-Based Mixed Phosphate Na ₄ Fe ₃ (PO ₄) ₂ P ₂ O ₇ Thin Films for Sodium-Ion Microbatteries. ACS Omega, 2020, 5, 7219-7224.	1.6	19
18	Different types of band alignment at MoS2/(Al, Ga, In)N heterointerfaces. Applied Physics Letters, 2020, 116	1.5	16

#	Article	IF	CITATIONS
19	Highly Responsive, Self-Powered <i>a</i> -GaN Based UV-A Photodetectors Driven by Unintentional Asymmetrical Electrodes. ACS Applied Electronic Materials, 2020, 2, 769-779.	2.0	31
20	Next-generation self-powered and ultrafast photodetectors based on III-nitride hybrid structures. APL Materials, 2020, 8, .	2.2	30
21	Highly photoresponsive VO2(M1) thin films synthesized by DC reactive sputtering. Journal of Materials Science: Materials in Electronics, 2020, 31, 4687-4695.	1.1	16
22	Enhanced humidity responsive ultrasonically nebulised V ₂ O ₅ thin films. Nano Express, 2020, 1, 010005.	1.2	13
23	Fabrication of smooth thin film of vanadium oxides (\$\$hbox {VO}_x\$\$) using pulsed laser deposition. Applied Physics A: Materials Science and Processing, 2020, 126, 1.	1.1	8
24	Fabrication of thin film electrode material by pulsed laser deposition. AIP Conference Proceedings, 2019, , .	0.3	0
25	Double Gaussian distribution of barrier heights and self-powered infrared photoresponse of InN/AIN/Si (111) heterostructure. Journal of Applied Physics, 2019, 126, .	1.1	19
26	NO ₂ gas sensing performance enhancement based on reduced graphene oxide decorated V ₂ O ₅ thin films. Nanotechnology, 2019, 30, 224001.	1.3	25
27	Highly Responsive ZnO/AlN/Si Heterostructure-Based Infrared- and Visible-Blind Ultraviolet Photodetectors With High Rejection Ratio. IEEE Transactions on Electron Devices, 2019, 66, 1345-1352.	1.6	17
28	Photodetection Properties of Nonpolar aâ€Plane GaN Grown by Three Approaches Using Plasmaâ€Assisted Molecular Beam Epitaxy. Physica Status Solidi (A) Applications and Materials Science, 2019, 216, 1900171.	0.8	17
29	A high-performance hydrogen sensor based on a reverse-biased MoS ₂ /GaN heterojunction. Nanotechnology, 2019, 30, 314001.	1.3	42
30	Low-cost VO ₂ (M1) thin films synthesized by ultrasonic nebulized spray pyrolysis of an aqueous combustion mixture for IR photodetection. RSC Advances, 2019, 9, 9983-9992.	1.7	24
31	Self-Powered, Broad Band, and Ultrafast InGaN-Based Photodetector. ACS Applied Materials & Interfaces, 2019, 11, 10418-10425.	4.0	61
32	Toward a Fast and Highly Responsive SnSe ₂ -Based Photodiode by Exploiting the Mobility of the Counter Semiconductor. ACS Applied Materials & Interfaces, 2019, 11, 6184-6194.	4.0	39
33	Preferentially oriented SrLi2Ti6O14 thin film anode for Li-ion micro-batteries fabricated by pulsed laser deposition. Electrochimica Acta, 2018, 269, 212-216.	2.6	6
34	Vis-Near-Infrared Photodetectors Based on Methyl Ammonium Lead Iodide Thin Films by Pulsed Laser Deposition. Journal of Electronic Materials, 2018, 47, 2306-2315.	1.0	4
35	In-Plane Anisotropic Photoconduction in Nonpolar Epitaxial <i>a</i> -Plane GaN. ACS Applied Materials & Interfaces, 2018, 10, 16918-16923.	4.0	33
36	Superior Electrochemical Performance of Amorphous Titanium Niobium Oxide Thin Films for Li-Ion Thin Film Batteries. Journal of the Electrochemical Society, 2018, 165, A764-A772.	1.3	12

#	Article	IF	CITATIONS
37	Gallium and indium co-doped ZnO as a transparent conducting oxide for Cu2SnS3 photodetectors. Journal of Materials Science: Materials in Electronics, 2018, 29, 2131-2139.	1.1	7
38	BTO/GaN heterostructure based on Schottky junction for high-temperature selective ultra-violet photo detection. Journal Physics D: Applied Physics, 2018, 51, 045104.	1.3	14
39	In-situ deposition of sodium titanate thin film as anode for sodium-ion micro-batteries developed by pulsed laser deposition. Journal of Colloid and Interface Science, 2018, 514, 117-121.	5.0	13
40	Temperature dependent electrical properties of AlN/Si heterojunction. Journal of Applied Physics, 2018, 124, 205111.	1.1	9
41	Reduced graphene oxide-based broad band photodetector and temperature sensor: effect of gas adsorption on optoelectrical properties. Journal of Nanoparticle Research, 2018, 20, 1.	0.8	14
42	Heterostructures of III-Nitride Semiconductors for Optical and Electronic Applications. , 2018, , .		2
43	Note: Simultaneous water quality monitoring and degradation of hazardous organic pollutants. Review of Scientific Instruments, 2018, 89, 096102.	0.6	5
44	Enhanced optical absorption of graphene-based heat mirror with tunable spectral selectivity. Solar Energy Materials and Solar Cells, 2018, 186, 149-153.	3.0	45
45	Wafer-scale synthesis of a uniform film of few-layer MoS ₂ on GaN for 2D heterojunction ultraviolet photodetector. Journal Physics D: Applied Physics, 2018, 51, 374003.	1.3	49
46	An Extrinsic Approach Toward Achieving Fast Response and Selfâ€Powered Photodetector. Physica Status Solidi (A) Applications and Materials Science, 2018, 215, 1800470.	0.8	20
47	An Overview of Nanostructured Li-based Thin Film Micro-batteries. Proceedings of the Indian National Science Academy, 2018, 98, .	0.5	7
48	Solvothermal Synthesis of Cu ₂ SnS ₃ Quantum Dots and Their Application in Near-Infrared Photodetectors. Inorganic Chemistry, 2017, 56, 2198-2203.	1.9	55
49	Heat-up synthesis of Cu ₂ SnS ₃ quantum dots for near infrared photodetection. RSC Advances, 2017, 7, 23301-23308.	1.7	26
50	Polarization-induced interfacial coupling modulations in BaTiO ₃ /GaN heterojunction devices. Journal Physics D: Applied Physics, 2017, 50, 275101.	1.3	10
51	Negative differential resistance and resistive switching in SnO2/ZnO interface. Journal of Applied Physics, 2017, 122, .	1.1	11
52	Reduced graphene oxide film based highly responsive infrared detector. Materials Research Express, 2017, 4, 085603.	0.8	8
53	Quantum Phase Transition in Few-Layer <mml:math <br="" xmlns:mml="http://www.w3.org/1998/Math/MathML">display="inline"><mml:mrow><mml:msub><mml:mrow><mml:mi>NbSe</mml:mi></mml:mrow><mml:mrow>< Probed through Quantized Conductance Fluctuations. Physical Review Letters, 2017, 119, 226802.</mml:mrow></mml:msub></mml:mrow></mml:math>	mm 1:0 nn>2	2<
54	Band Gap Engineering of Hexagonal SnSe2 Nanostructured Thin Films for Infra-Red Photodetection. Scientific Reports, 2017, 7, 15215.	1.6	102

#	Article	IF	CITATIONS
55	Sequential Elemental Dealloying Approach for the Fabrication of Porous Metal Oxides and Chemiresistive Sensors Thereof for Electronic Listening. ACS Applied Materials & Interfaces, 2017, 9, 41428-41434.	4.0	27
56	Effect of Illumination Intensities on the Visible and Infrared Photoresponse of Cu2SnS3 Nanostructures. Journal of Nanoscience and Nanotechnology, 2017, 17, 413-419.	0.9	5
57	Mechanistic view on efficient photodetection by solvothermally reduced graphene oxide. Journal of Materials Science: Materials in Electronics, 2017, 28, 14818-14826.	1.1	9
58	Experimental evidence on RH-dependent crossover from an electronic to protonic conduction with an oscillatory behaviour. Applied Physics Letters, 2017, 110, .	1.5	15
59	Na2Ti6O13 thin films as anode for thin film sodium ion batteries. AIP Conference Proceedings, 2017, , .	0.3	2
60	Enhanced UV Photodetector Response of ZnO/Si With AlN Buffer Layer. IEEE Transactions on Electron Devices, 2017, 64, 4161-4166.	1.6	25
61	Deep UV-Vis photodetector based on ferroelectric/semiconductor heterojunction. Journal of Applied Physics, 2017, 122, .	1.1	19
62	Solution-Cast Photoconductive Photodetectors Based on CulnSe ₂ Nanoparticles. Journal of Nanoscience and Nanotechnology, 2017, 17, 1538-1542.	0.9	5
63	Role of component layers in designing carbon nanotubes-based tandem absorber on metal substrates for solar thermal applications. Solar Energy Materials and Solar Cells, 2016, 155, 397-404.	3.0	8
64	Solution processed Cu2SnS3 thin films for visible and infrared photodetector applications. AIP Advances, 2016, 6, .	0.6	48
65	Cu2SnS3nanostructures for inorganic–organic hybrid infrared photodetector applications. Materials Research Express, 2016, 3, 105006.	0.8	9
66	Controlled growth of high-quality graphene using hot-filament chemical vapor deposition. Applied Physics A: Materials Science and Processing, 2016, 122, 1.	1.1	8
67	Understanding Pt–ZnO:In Schottky nanocontacts by conductive atomic force microscopy. Materials Research Express, 2016, 3, 045023.	0.8	4
68	Fabrication of TiNb2O7 thin film electrodes for Li-ion micro-batteries by pulsed laser deposition. Materials Science and Engineering B: Solid-State Materials for Advanced Technology, 2016, 213, 90-97.	1.7	27
69	InN Quantum Dot Based Infra-Red Photodetectors. Journal of Nanoscience and Nanotechnology, 2016, 16, 709-714.	0.9	11
70	Structural and optical characterization of nonpolar (10–10) m-InN/m-GaN epilayers grown by PAMBE. Journal of Crystal Growth, 2016, 433, 74-79.	0.7	5
71	Cu2SnS3 Inorganic-Organic Hybrid Structures for Photovoltaic Applications. Materials Research Society Symposia Proceedings, 2015, 1784, 1.	0.1	1
72	Determination of band offsets at the Al:ZnO/Cu2SnS3 interface using X-ray photoelectron spectroscopy. AlP Advances, 2015, 5, .	0.6	9

#	Article	IF	CITATIONS
73	Enhanced UV detection by non-polar epitaxial GaN films. AIP Advances, 2015, 5, .	0.6	31
74	Temperature dependent electrical characterisation of Pt/HfO2/n-GaN metal-insulator-semiconductor (MIS) Schottky diodes. AIP Advances, 2015, 5, .	0.6	54
75	Impact of Nitridation on Structural and Optical Properties of Epitaxial GaN Films Grown on M-Plane Sapphire by PAMBE. Materials Research Society Symposia Proceedings, 2015, 1736, 76.	0.1	1
76	Nanocomposite Based Organic–Inorganic Cu ₃ BiS ₃ High Sensitive Hybrid Photonic Devices. Journal of Nanoscience and Nanotechnology, 2015, 15, 2742-2752.	0.9	7
77	Study of band offsets at the Cu2SnS3/In2O3: Sn interface using x-ray photoelectron spectroscopy. Materials Research Express, 2015, 2, 065901.	0.8	4
78	Solution processible Cu 2 SnS 3 thin films for cost effective photovoltaics: Characterization. Materials Chemistry and Physics, 2015, 167, 309-314.	2.0	24
79	Observation of Room Temperature Ferromagnetism in InN Nanostructures. Journal of Nanoscience and Nanotechnology, 2015, 15, 4426-4430.	0.9	7
80	Transport properties of solution processed Cu2SnS3/AZnO heterostructure for low cost photovoltaics. Solar Energy Materials and Solar Cells, 2015, 143, 152-158.	3.0	38
81	Preferential polarization and its reversal in polycrystalline BiFeO3/La0.5Sr0.5CoO3 heterostructures. Solid State Communications, 2015, 208, 15-20.	0.9	4
82	Growth and electrical transport properties of InGaN/GaN heterostructures grown by PAMBE. Materials Research Bulletin, 2015, 61, 539-543.	2.7	9
83	High indium non-polar InGaN clusters with infrared sensitivity grown by PAMBE. AIP Advances, 2015, 5, 037112.	0.6	8
84	Binary group III-nitride based heterostructures: band offsets and transport properties. Journal Physics D: Applied Physics, 2015, 48, 423001.	1.3	62
85	Trap modulated photoresponse of InGaN/Si isotype heterojunction at zero-bias. Journal of Applied Physics, 2015, 118, .	1.1	19
86	Barrier height inhomogeneity in electrical transport characteristics of InGaN/GaN heterostructure interfaces. AIP Advances, 2015, 5, .	0.6	16
87	An insight to the low temperature conduction mechanism ofc-axis grown Al-doped ZnO, a widely used transparent conducting oxide. Journal Physics D: Applied Physics, 2015, 48, 015301.	1.3	10
88	Culn1â^'xAlxSe2 Thin Films Grown by Co-Sputtering and Modified Selenization: Application in Flexible Solar Cells. IEEE Journal of the Electron Devices Society, 2015, 3, 244-253.	1.2	2
89	Plasmonic enhancement of photocurrent in GaN based UV photodetectors. , 2014, , .		9
90	Semipolar and nonpolar GaN epi-films grown on m-sapphire by plasma assisted molecular beam epitaxy. Journal of Applied Physics, 2014, 116, .	1.1	38

#	Article	IF	CITATIONS
91	Near-infrared photoactive Cu3BiS3 thin films by co-evaporation. Journal of Applied Physics, 2014, 115, .	1.1	25
92	Growth and Characterization of a-plane In0.2Ga0.8N/ GaN hetrostructures on r-Sapphire. Materials Research Society Symposia Proceedings, 2014, 1736, 31.	0.1	0
93	Pt/n-GaN metal-semiconductor and Pt/HfO2/n-GaN metal-insulator-semiconductor Schottky diodes. Materials Research Society Symposia Proceedings, 2014, 1736, 7.	0.1	0
94	Smart Materials for Energy Harvesting, Energy Storage, and Energy Efficient Solid-State Electronic Refrigeration. Springer Tracts in Mechanical Engineering, 2014, , 303-315.	0.1	1
95	Study of InN nanorods growth mechanism using ultrathin Au layer by plasma-assisted MBE on Si(111). Applied Nanoscience (Switzerland), 2014, 4, 121-125.	1.6	2
96	Temperature dependent electrical behaviour of Cu2SnS3 films. AIP Advances, 2014, 4, 037121.	0.6	10
97	Transport properties of Culn _{1â^'x} Al _x Se ₂ /AZnO heterostructure for low cost thin film photovoltaics. Dalton Transactions, 2014, 43, 1974-1983.	1.6	29
98	Effects of growth temperature on nonpolar aâ€plane InN grown by molecular beam epitaxy. Physica Status Solidi C: Current Topics in Solid State Physics, 2014, 11, 932-935.	0.8	3
99	Fabrication of large-area PbSe films at the organic–aqueous interface and their near-infrared photoresponse. Journal of Materials Chemistry C, 2014, 2, 6283.	2.7	10
100	Carbon Nanotubeâ€Based Tandem Absorber with Tunable Spectral Selectivity: Transition from Nearâ€Perfect Blackbody Absorber to Solar Selective Absorber. Advanced Materials, 2014, 26, 2552-2557.	11.1	95
101	Solution Processed Cu ₂ CoSnS ₄ Thin Films for Photovoltaic Applications. Crystal Growth and Design, 2014, 14, 3685-3691.	1.4	63
102	Double Gaussian distribution of barrier height observed in densely packed GaN nanorods over Si (111) heterostructures. Journal of Applied Physics, 2014, 116, .	1.1	8
103	Impact of substrate nitridation on the photoluminescence and photovoltaic characteristics of GaN grown on p-Si (100) by molecular beam epitaxy. Journal of Materials Science: Materials in Electronics, 2013, 24, 3371-3375.	1.1	1
104	Anomalous magnetic behavior of La0.6Sr0.4MnO3 nano-tubes constituted with 3–12 nm particles. Applied Physics A: Materials Science and Processing, 2013, 111, 605-612.	1.1	15
105	Facile synthesis of Cu2CoSnS4 nanoparticles exhibiting red-edge-effect: Application in hybrid photonic devices. Journal of Applied Physics, 2013, 114, .	1.1	61
106	Near infrared detectors based on HgSe and HgCdSe quantum dots generated at the liquid–liquid interface. Journal of Materials Chemistry C, 2013, 1, 6184.	2.7	36
107	Substrate impact on the growth of InN nanostructures by droplet epitaxy. Physica Status Solidi C: Current Topics in Solid State Physics, 2013, 10, 409-412.	0.8	4
108	Low dimensional fabrication of giant dielectric CaCu3Ti4O12 through soft e-beam lithography. Journal of Alloys and Compounds, 2013, 547, 147-151.	2.8	14

#	Article	IF	CITATIONS
109	Electrical transport studies of MBE grown InGaN/Si isotype heterojunctions. Current Applied Physics, 2013, 13, 26-30.	1.1	13
110	Spectroscopic Studies of In ₂ O ₃ Nanostructures; Photovoltaic Demonstration of In ₂ O ₃ /p-Si Heterojunction. Journal of Nanoscience and Nanotechnology, 2013, 13, 498-503.	0.9	4
111	Sol-gel processed Cu[sub 2]SnS[sub 3] films for photovoltaics. , 2013, , .		1
112	Electrical and Optical Properties of Electron Irradiated ZnO: Li Thin Films. Advanced Materials Research, 2013, 699, 257-261.	0.3	1
113	Molecular beam epitaxial growth of (1 1 -2 2) GaN on m-plane sapphire. Physica Status Solidi C: Current Topics in Solid State Physics, 2013, 10, 381-384.	0.8	1
114	Culn <inf>1−x</inf> Al <inf>x</inf> Se <inf>2</inf> solar cells fabricated on the flexible substrates by co-sputtering and modified selenization. , 2013, , .		0
115	Electrocaloric Effect in 0.85PMN-0.15PT Thin Films Deposited by Pulsed Laser Deposition. Ferroelectrics, 2013, 453, 38-43.	0.3	3
116	Near-infrared photoactive Cu2ZnSnS4 thin films by co-sputtering. AIP Advances, 2013, 3, .	0.6	32
117	Tailoring the Cu(In, Al)S <inf>2</inf> nanostructures for photonic applications. , 2013, , .		3
118	Tailoring the Band Gap and Transport Properties of Cu ₃ BiS ₃ Nanopowders for Photodetector Applications. Journal of Nanoscience and Nanotechnology, 2013, 13, 3901-3909.	0.9	13
119	Comparative studies on photovoltaic performance of InN nanostructures/p-Si(100) heterojunction devices grown by molecular beam epitaxy. Materials Research Society Symposia Proceedings, 2012, 1391, 95.	0.1	1
120	Molecular Beam Epitaxial Growth of Nonpolar a-plane InN/ GaN Heterostructures. Materials Research Society Symposia Proceedings, 2012, 1396, .	0.1	0
121	Growth and study of CuIn1-xAlxSe2 thin films for photovoltaic applications. , 2012, , .		Ο
122	Current transport in nonpolar a-plane InN/GaN heterostructures Schottky junction. Journal of Applied Physics, 2012, 112, 023706.	1.1	15
123	Unusual photoresponse of indium doped ZnO/organic thin film heterojunction. Applied Physics Letters, 2012, 100, .	1.5	62
124	Structural Characterization and Ultraviolet Photoresponse of GaN Nanodots Grown by Molecular Beam Epitaxy. Applied Physics Express, 2012, 5, 085202.	1.1	10
125	Studies on Field Dependent Domain Structures in Multi-Grained 0.85PbMg _{1/3} Nb _{2/3} O3–0.15PbTiO ₃ Thin Films by Scanning Force Microscopy. Integrated Ferroelectrics, 2012, 134, 39-47.	0.3	1
126	Band-Structure Lineup at In\$_{0.2}\$Ga\$_{0.8}\$N/Si Heterostructures by X-ray Photoelectron Spectroscopy. Japanese Journal of Applied Physics, 2012, 51, 020203.	0.8	2

#	Article	IF	CITATIONS
127	Tuning the photoluminescence of ZnO thin films by indium doping. , 2012, , .		0
128	Growth and properties of nonpolar a-plane GaN grown on r-sapphire by plasma assisted molecular beam epitaxy. Proceedings of SPIE, 2012, , .	0.8	0
129	Wurtzite InN nanodots on Si(100) by molecular beam epitaxy. Proceedings of SPIE, 2012, , .	0.8	0
130	Solution-based synthesis of cobalt-doped ZnO thin films. Thin Solid Films, 2012, 524, 137-143.	0.8	45
131	Effect of carrier concentration of InN on the transport behavior of InN/GaN heterostructure based Schottky junctions. Solid State Communications, 2012, 152, 1771-1775.	0.9	2
132	Indium flux, growth temperature and RF power induced effects in InN layers grown on GaN/Si substrate by plasma-assisted MBE. Journal of Alloys and Compounds, 2012, 513, 6-9.	2.8	9
133	Cobalt-doped ZnO nanowires on quartz: Synthesis by simple chemical method and characterization. Journal of Crystal Growth, 2012, 343, 7-12.	0.7	30
134	Influence of GaN underlayer thickness on structural, electrical and optical properties of InN films grown by PAMBE. Journal of Crystal Growth, 2012, 354, 208-211.	0.7	10
135	Large nonlinear refraction and two photon absorption in ferroelectric Bi2VO5.5 thin films. Optical Materials, 2012, 34, 1822-1825.	1.7	9
136	Synthesis and structural characterization of two-dimensional hierarchical covellite nano-structures. Materials Chemistry and Physics, 2012, 137, 466-471.	2.0	17
137	Perovskite phase transformation in 0.65Pb(Mg1/3Nb2/3)O3-0.35PbTiO3 nanoparticles derived by sol-gel. Journal of Applied Physics, 2012, 111, 024314.	1.1	4
138	Gallium and indium coâ€doped ZnO thin films for white light emitting diodes. Physica Status Solidi - Rapid Research Letters, 2012, 6, 34-36.	1.2	20
139	Determination of MBE grown wurtzite GaN/Ge ₃ N ₄ /Ge heterojunctions band offset by Xâ€ғay photoelectron spectroscopy. Physica Status Solidi (B): Basic Research, 2012, 249, 58-61.	0.7	19
140	Carrierâ€transport studies of IIIâ€nitride/Si ₃ N ₄ /Si isotype heterojunctions. Physica Status Solidi (A) Applications and Materials Science, 2012, 209, 994-997.	0.8	9
141	Analysis of the temperature-dependent current-voltage characteristics and the barrier-height inhomogeneities of Au/GaN Schottky diodes. Physica Status Solidi (A) Applications and Materials Science, 2012, 209, 1575-1578.	0.8	12
142	Novel Radiationâ€Induced Properties of Graphene and Related Materials. Macromolecular Chemistry and Physics, 2012, 213, 1146-1163.	1.1	67
143	Carrier concentration dependence of donor activation energy in n-type GaN epilayers grown on Si (111) by plasma-assisted MBE. Materials Research Bulletin, 2012, 47, 1306-1309.	2.7	11
144	Valence band offset at GaN/β-Si3N4 and β-Si3N4/Si(111) heterojunctions formed by plasma-assisted molecular beam epitaxy. Thin Solid Films, 2012, 520, 4911-4915.	0.8	13

#	Article	IF	CITATIONS
145	Study of n-ZnO/p-Si (100) thin film heterojunctions by pulsed laser deposition without buffer layer. Thin Solid Films, 2012, 520, 5894-5899.	0.8	64
146	Solvothermal Synthesis, Structural and Optical Properties of Phase-Pure Cu ₃ BiS ₃ Nano-Powders Exhibiting Near-IR Photodetection. Advanced Science, Engineering and Medicine, 2012, 4, 89-95.	0.3	3
147	Band-Structure Lineup at In0.2Ga0.8N/Si Heterostructures by X-ray Photoelectron Spectroscopy. Japanese Journal of Applied Physics, 2012, 51, 020203.	0.8	1
148	Solution processed reduced graphene oxide ultraviolet detector. Applied Physics Letters, 2011, 99, .	1.5	101
149	Substrate nitridation induced modulations in transport properties of wurtzite GaN/p-Si (100) heterojunctions grown by molecular beam epitaxy. Journal of Applied Physics, 2011, 110, .	1.1	21
150	Experimental evidence of Ga-vacancy induced room temperature ferromagnetic behavior in GaN films. Applied Physics Letters, 2011, 99, 162512.	1.5	45
151	Size dependent bandgap of molecular beam epitaxy grown InN quantum dots measured by scanning tunneling spectroscopy. Journal of Applied Physics, 2011, 110, 114317.	1.1	9
152	An aqueous-solution based low-temperature pathway to synthesize giant dielectric CaCu3Ti4O12—Highly porous ceramic matrix and submicron sized powder. Journal of Alloys and Compounds, 2011, 509, 4381-4385.	2.8	20
153	Structural and dielectric behavior of pulsed laser ablated Sr0.6Ca0.4TiO3 thin film and asymmetric multilayer of SrTiO3 and CaTiO3. Journal of Crystal Growth, 2011, 337, 7-12.	0.7	3
154	Indium Nitride (InN) Nanostructures Grown by Plasma-Assisted Molecular Beam Epitaxy (PAMBE). , 2011, , ,		0
155	Effect of N/Ga flux ratio on transport behavior of Pt/GaN Schottky diodes. Journal of Applied Physics, 2011, 110, .	1.1	8
156	Barrier height inhomogeneities in InN/GaN heterostructure based Schottky junctions. Solid State Communications, 2011, 151, 1420-1423.	0.9	15
157	Structural and optical properties of nonpolar (11â^20) a-plane GaN grown on (1â^2102) r-plane sapphire substrate by plasma-assisted molecular beam epitaxy. Scripta Materialia, 2011, 65, 33-36.	2.6	15
158	Synthesis, structural characterization and ferroelectric properties of Pb0.76Ca0.24TiO3 nanotubes. Materials Chemistry and Physics, 2011, 131, 443-448.	2.0	5
159	Growth of InN layers on Si (111) using ultra thin silicon nitride buffer layer by NPA-MBE. Materials Letters, 2011, 65, 1396-1399.	1.3	20
160	Structural and electrical studies on Bi2VO5.5/Bi4Ti3O12 multilayer thin films. Journal of Materials Science: Materials in Electronics, 2011, 22, 639-648.	1.1	3
161	Kinetics of self-assembled InN quantum dots grown on Si (111) by plasma-assisted MBE. Journal of Nanoparticle Research, 2011, 13, 1281-1287.	0.8	11
162	Reduction of oxygen impurity at GaN/β-Si3N4/Si interface via SiO2 to Ga2O conversion by exposing of Si surface under Ga flux. Journal of Crystal Growth, 2011, 327, 272-275.	0.7	4

#	Article	IF	CITATIONS
163	Synthesis and structural characterization of perovskite 0.65Pb(Mg1/3Nb2/3)O3–0.35PbTiO3 nanotubes. Physics Letters, Section A: General, Atomic and Solid State Physics, 2011, 375, 2176-2180.	0.9	6
164	Transport and infrared photoresponse properties of InN nanorods/Si heterojunction. Nanoscale Research Letters, 2011, 6, 609.	3.1	24
165	Evidences for ambient oxidation of indium nitride quantum dots. Physica Status Solidi (B): Basic Research, 2011, 248, 2853-2856.	0.7	4
166	Infrared Photodetectors Based on Reduced Graphene Oxide and Graphene Nanoribbons. Advanced Materials, 2011, 23, 5419-5424.	11.1	297
167	The impact of ultra thin silicon nitride buffer layer on GaN growth on Si (111) by RF-MBE. Applied Surface Science, 2011, 257, 2107-2110.	3.1	8
168	Multilayer Bi1.5Zn1.0Nb1.5O7/Ba0.6Sr0.4TiO3/Bi1.5Zn1.0Nb1.5O7 thin films for tunable microwave applications. Applied Surface Science, 2011, 257, 2214-2217.	3.1	17
169	Temperature-dependent photoluminescence of GaN grown on β-Si3N4/Si (111) by plasma-assisted MBE. Journal of Luminescence, 2011, 131, 614-619.	1.5	11
170	Pulsed laser deposited ZnO/ZnO:Li multilayer for blue light emitting diodes. Journal of Luminescence, 2011, 131, 1649-1654.	1.5	10
171	Electroluminescence from GaN–polymer heterojunction. Journal of Luminescence, 2011, 131, 2612-2615.	1.5	4
172	Growth temperature induced effects in non-polar a-plane GaN on r-plane sapphire substrate by RF-MBE. Journal of Crystal Growth, 2011, 314, 5-8.	0.7	16
173	Negative differential capacitance in n-GaN/p-Si heterojunctions. Solid State Communications, 2011, 151, 356-359.	0.9	14
174	Study of band offsets in InN/Ge heterojunctions. Surface Science, 2011, 605, L33-L37.	0.8	3
175	Pulsed laser deposited ZnO:In as transparent conducting oxide. Thin Solid Films, 2011, 519, 3647-3652.	0.8	18
176	Effect of oxygen pressure on the grain and domain structure of polycrystalline 0.85PbMg1/3Nb2/3O3–0.15PbTiO3thin films studied by scanning probe microscopy. Journal Physics D: Applied Physics, 2011, 44, 415401.	1.3	3
177	Band alignment studies in InN/p-Si(100) heterojunctions by x-ray photoelectron spectroscopy. Journal of Applied Physics, 2011, 109, .	1.1	18
178	Temperature dependent transport studies in InN quantum dots grown by droplet epitaxy on silicon nitride/Si substrate. Applied Physics Letters, 2011, 99, 153114.	1.5	12
179	Temperature dependent electrical transport behavior of InN/GaN heterostructure based Schottky diodes. Journal of Applied Physics, 2011, 109, 044502-044502-5.	1.1	25
180	Barrier Inhomogeneity and Electrical Properties of InN Nanodots/Si Heterojunction Diodes. Journal of Nanomaterials, 2011, 2011, 1-7.	1.5	5

#	Article	IF	CITATIONS
181	Antiferroelectric Phase Transition in PbZrO ₃ Nanoparticles. Advanced Science Letters, 2011, 4, 3599-3601.	0.2	0
182	Polarization enhancement in compositionally graded vanadium doped bismuth titanate thin films. Journal of Applied Physics, 2010, 107, .	1.1	8
183	Indium Nitride Nanometric-Objects on c-Sapphire Grown by Plasma-Assisted Molecular Beam Epitaxy. Nanoscience and Nanotechnology Letters, 2010, 2, 257-260.	0.4	1
184	Studies on effect of dielectric coating on the triple junction electric field in ferroelectric cathodes. , 2010, , .		0
185	Dielectric properties of electron irradiated PbZrO3 thin films. Bulletin of Materials Science, 2010, 33, 191-196.	0.8	5
186	Self-assembled flower-like nanostructures of InN and GaN grown by plasma-assisted molecular beam epitaxy. Bulletin of Materials Science, 2010, 33, 221-226.	0.8	17
187	Structural, optical and electrical characteristics of transparent bismuth vanadate films deposited on indium tin oxide coated glass substrates. Journal of Materials Science: Materials in Electronics, 2010, 21, 1107-1114.	1.1	6
188	ZnO nanocrystalline thin films: a correlation of microstructural, optoelectronic properties. Journal of Materials Science: Materials in Electronics, 2010, 21, 355-359.	1.1	20
189	Spectroscopic ellipsometry investigations of the optical properties of manganese doped bismuth vanadate thin films. Materials Research Bulletin, 2010, 45, 464-473.	2.7	5
190	Improved growth of GaN layers on ultra thin silicon nitride/Si (111) by RF-MBE. Materials Research Bulletin, 2010, 45, 1581-1585.	2.7	27
191	Impedance studies on high energy Li3+ irradiated PZT thin films. Nuclear Instruments & Methods in Physics Research B, 2010, 268, 476-480.	0.6	0
192	Investigation of true remnant polarization response in heterostructured artificial biferroics. Solid State Communications, 2010, 150, 660-662.	0.9	9
193	Characteristics of field-effect transistors based on undoped and B- and N-doped few-layer graphenes. Solid State Communications, 2010, 150, 734-738.	0.9	60
194	Effect of La modification on antiferroelectricity and dielectric phase transition in sol–gel grown thin films. Solid State Communications, 2010, 150, 1755-1759.	0.9	11
195	Room-temperature gas sensors based on gallium nitride nanoparticles. Solid State Communications, 2010, 150, 2053-2056.	0.9	56
196	Probing disorder in cubic pyrochlore Bi1.5Zn1.0Nb1.5O7 (BZN) thin films. Solid State Communications, 2010, 150, 2257-2261.	0.9	7
197	Temperature dependent transport behavior of n-InN nanodot/p-Si heterojunction structures. Applied Physics Letters, 2010, 97, 202107.	1.5	16
198	Wide Ranged La Modification in CCTO Ceramics Through Sol-Gel: Effect on Microstructure and Dielectric Properties. Integrated Ferroelectrics, 2010, 121, 86-98.	0.3	4

#	Article	IF	CITATIONS
199	High-temperature dielectric response in pulsed laser deposited Bi1.5Zn1.0Nb1.5O7 thin films. Journal of Applied Physics, 2010, 108, .	1.1	10
200	Low Temperature Synthesis of Nano-Crystalline CaCu3Ti4O12 Through a Fuel Mediated Auto-Combustion Pathway. Current Nanoscience, 2010, 6, 432-438.	0.7	9
201	A Comparative Study of the Effect of Metallic Au and ReO3Nanoparticles on the Performance of Silicon Solar Cells. Applied Physics Express, 2010, 3, 115001.	1.1	0
202	Facile hydrothermal synthesis and observation of bubbled growth mechanism in nano-ribbons aggregated microspherical Covellite blue-phosphor. Dalton Transactions, 2010, 39, 9789.	1.6	37
203	Synthesis and Studies of Pb ₀ . ₇₆ Ca ₀ . ₂₄ TiO ₃ Nanoparticles Derived by Sol–Gel. Advanced Science Letters, 2010, 3, 363-367.	0.2	1
204	Droplet Epitaxy of InN Quantum Dots on Si(111) by RF Plasma-Assisted Molecular Beam Epitaxy. Advanced Science Letters, 2010, 3, 379-384.	0.2	15
205	Structural and electrical characterization of Bi2VO5.5 / Bi4Ti3O12 bilayer thin films deposited by pulsed laser ablation technique. Natural Science, 2010, 02, 1073-1078.	0.2	4
206	Investigation of biferroic properties in La0.6Sr0.4MnO3/0.7Pb(Mg1/3Nb2/3)O3–0.3PbTiO3 epitaxial bilayered heterostructures. Journal of Applied Physics, 2009, 106, .	1.1	14
207	Fabrication, Structural Characterization, and Formation Mechanism of Ferroelectric SrBi ₂ Ta ₂ O ₉ Nanotubes. Nanoscience and Nanotechnology Letters, 2009, 1, 8-12.	0.4	1
208	Synthesis, Structural Characterization and Formation Mechanism of Ferroelectric Bismuth Vanadate Nanotubes. Journal of Nanoscience and Nanotechnology, 2009, 9, 6549-6553.	0.9	6
209	Electrocaloric effect of PMN-PT thin films near morphotropic phase boundary. Bulletin of Materials Science, 2009, 32, 259-262.	0.8	127
210	Assembly of sol–gel-grown Li x CoO2 nanocrystals throughÂelectromagnetic irradiation. Applied Physics A: Materials Science and Processing, 2009, 95, 523-536.	1.1	1
211	Negative differential resistance in GaN nanocrystals above room temperature. Nanotechnology, 2009, 20, 405205.	1.3	15
212	Sol-Gel Template Synthesis, Structural Characterization and Growth Mechanism of Barium Zirconate Nanotubes. Current Nanoscience, 2009, 5, 339-343.	0.7	8
213	Synthesis of One-Dimensional ZnO Nanostructures from Zn Powder/Granule. Journal of Nanoscience and Nanotechnology, 2009, 9, 2061-2065.	0.9	4
214	Fabrication and Phase Transformation in Crystalline Nanoparticles of PbZrO3 Derived By Sol-Gel. Current Nanoscience, 2009, 5, 489-492.	0.7	3
215	Structural, ferroelectric and optical properties of Bi2VO5.5 thin films deposited on platinized silicon {(100) Pt/TiO2/SiO2/Si} substrates. Applied Physics A: Materials Science and Processing, 2008, 91, 693-699.	1.1	17
216	Structural, optical and ac conduction properties of Bi2V1â^'xNbxO5.5 (0≤â‰ੳ.4) thin films fabricated by pulsed laser deposition technique. Materials Science and Engineering B: Solid-State Materials for Advanced Technology, 2008, 153, 36-46.	1.7	8

#	Article	IF	CITATIONS
217	Magnetocapacitive La0.6Sr0.4MnO3 /0.7Pb(Mg1 / 3Nb2 / 3)O3–0.3PbTiO3 epitaxial heterostructure. Solid State Communications, 2008, 148, 566-569.	0.9	7
218	The structural and electrical properties of TiO2 thin films prepared by thermal oxidation. Physica B: Condensed Matter, 2008, 403, 3718-3723.	1.3	42
219	Electrocaloric effect in antiferroelectric PbZrO ₃ thin films. Physica Status Solidi - Rapid Research Letters, 2008, 2, 230-232.	1.2	61
220	Surface spin glass behavior in sol–gel derived La0.7Ca0.3MnO3 nanotubes. Dalton Transactions, 2008, , 4708.	1.6	11
221	Dielectric response of BaZrO3/BaTiO3 and SrTiO3/BaZrO3 superlattices. Journal of Applied Physics, 2008, 104, .	1.1	19
222	Enhancement of charge and energy storage in sol-gel derived pure and La-modified PbZrO3 thin films. Applied Physics Letters, 2008, 92, 192901.	1.5	128
223	Constrained ferroelectricity in BaTiO3â^•BaZrO3 superlattices. Applied Physics Letters, 2008, 92, .	1.5	14
224	dc leakage mechanism in artificial biferroic superlattices. Journal of Applied Physics, 2008, 104, .	1.1	5
225	Slim P-E hysteresis loop and anomalous dielectric response in sol-gel derived antiferroelectric PbZrO3 thin films. Journal of Applied Physics, 2008, 104, .	1.1	9
226	Lead Zirconate Nanotubes: Synthesis, Structural Characterization and Growth Mechanism. Journal of Nanoscience and Nanotechnology, 2008, 8, 5757-5761.	0.9	3
227	Fabrication, Structural Characterization and Formation Mechanism of Multiferroic BiFeO ₃ Nanotubes. Journal of Nanoscience and Nanotechnology, 2008, 8, 335-339.	0.9	17
228	X-Ray Diffraction & Residual Stresses in Ferroelectric Cathodes. , 2007, , .		0
229	Off-centered polarization and ferroelectric phase transition in Li-doped ZnO thin films grown by pulsed-laser ablation. Journal of Applied Physics, 2007, 101, 104104.	1.1	44
230	Antiferroelectriclike polarization behavior in compositionally varying (1â^'x)â€^Pb(Mg1â^•3Nb2â^•3)O3–(x)â€^Pb multilayers. Applied Physics Letters, 2007, 91, .	oTjQ3	14
231	Role of template layer on microstructure, phase formation and polarization behavior of ferroelectric relaxor thin films. Journal of Applied Physics, 2007, 101, 104111.	1.1	6
232	Ferroelectric interaction and polarization studies in BaTiO3â^•SrTiO3 superlattice. Journal of Applied Physics, 2007, 101, 104113.	1.1	20
233	Leakage current behavior in pulsed laser deposited Ba(Zr0.05Ti0.95)O3 thin films. Journal of Applied Physics, 2007, 101, 034106.	1.1	37
234	Realization of biferroic properties in La0.6Sr0.4MnO3â^•0.7Pb(Mg1â^•3Nb2â^•3)O3–0.3(PbTiO3) epitaxial superlattices. Journal of Applied Physics, 2007, 101, 114104.	1.1	12

#	Article	IF	CITATIONS
235	Improved ferroelectric and leakage properties in symmetric BiFeO3â^•SrTiO3 superlattice. Applied Physics Letters, 2007, 90, 212902.	1.5	34
236	Engineered Biferroic 0.7Pb(Mg1/3Nb2/3)O3-0.3PbTiO3/La0.6Sr0.4MnO3 Epitaxial Superlattices. Materials Research Society Symposia Proceedings, 2007, 1034, 50.	0.1	0
237	Interface dominated biferroic La0.6Sr0.4MnO3â^•0.7Pb(Mg1â^•3Nb2â^•3)O3–0.3PbTiO3 epitaxial superlattices. Applied Physics Letters, 2007, 90, 122902.	1.5	39
238	Low threshold voltage ZnO thin film transistor with a Zn0.7Mg0.3O gate dielectric for transparent electronics. Journal of Applied Physics, 2007, 101, .	1.1	50
239	Nonlinear dielectric behavior in three-component ferroelectric superlattices. Journal of Applied Physics, 2007, 102, 024108.	1.1	8
240	Studies on strontium titanate/barium zirconate superlattices. Solid State Communications, 2007, 143, 223-227.	0.9	1
241	Study of three-component ferroelectric perovskite superlattices. Solid State Communications, 2007, 143, 510-514.	0.9	4
242	Investigations on zinc oxide thin films grown on Si (100) by thermal oxidation. Materials Science and Engineering B: Solid-State Materials for Advanced Technology, 2007, 137, 126-130.	1.7	14
243	Dielectric, impedance and ferroelectric characteristics of c-oriented bismuth vanadate films grown by pulsed laser deposition. Materials Science and Engineering B: Solid-State Materials for Advanced Technology, 2007, 138, 22-30.	1.7	35
244	ac conductivity studies on the electron irradiated BaZrO3 ceramic. Nuclear Instruments & Methods in Physics Research B, 2007, 257, 505-509.	0.6	21
245	High energy oxygen ion induced modifications in lead based perovskite thin films. Nuclear Instruments & Methods in Physics Research B, 2007, 260, 553-562.	0.6	3
246	Investigations on magnetron sputtered ZnO thin films and Au/ZnO Schottky diodes. Physica B: Condensed Matter, 2007, 391, 344-349.	1.3	43
247	Synthesis and structural characterization of Ba0.6Sr0.4TiO3 nanotubes. Physics Letters, Section A: General, Atomic and Solid State Physics, 2007, 367, 356-359.	0.9	26
248	Synthesis and structural characterization of the antiferroelectric lead zirconate nanotubes by pulsed laser deposition. Applied Physics A: Materials Science and Processing, 2007, 87, 27-30.	1.1	17
249	Dielectric anomaly in Li-doped zinc oxide thin films grown by sol–gel route. Applied Physics A: Materials Science and Processing, 2007, 88, 421-424.	1.1	18
250	Growth of ferroelectric Li-doped ZnO thin films for metal-ferroelectric-semiconductor FET. Journal Physics D: Applied Physics, 2006, 39, 2664-2669.	1.3	27
251	Interfacial coupling and its size dependence inPbTiO3andPbMg1â^•3Nb2â^•3O3multilayers. Physical Review B, 2006, 74, .	1.1	32
252	Growth and transport properties of CuInSe2/ZnO heterostructure solar cell. Materials Science and Engineering B: Solid-State Materials for Advanced Technology, 2006, 127, 12-16.	1.7	14

#	Article	IF	CITATIONS
253	dc and ac transport properties of Mn-doped ZnO thin films grown by pulsed laser ablation. Materials Science and Engineering B: Solid-State Materials for Advanced Technology, 2006, 133, 70-76.	1.7	37
254	Temperature dependent transport properties of CuInSe2–ZnO heterostructure solar Cell. Journal of Physics and Chemistry of Solids, 2006, 67, 1636-1642.	1.9	7
255	C–V studies on metal–ferroelectric bismuth vanadate (Bi2VO5.5)–semiconductor structure. Solid State Communications, 2006, 137, 566-569.	0.9	22
256	Ferroelectricity in (M=Al and Ga) with the structure. Solid State Communications, 2006, 140, 42-44.	0.9	12
257	First Indo-Singapore Symposium on "Advanced Functional Materialsâ€ , Mumbai, 2006. Bulletin of Materials Science, 2006, 29, 547-547.	0.8	0
258	Dielectric properties of (110) oriented PbZrO3 and La-modified PbZrO3 thin films grown by sol-gel process on Pt(111)â^•Tiâ^•SiO2â^•Si substrate. Journal of Applied Physics, 2006, 100, 044102.	1.1	28
259	Effect of Li substitution on dielectric and ferroelectric properties of ZnO thin films grown by pulsed-laser ablation. Journal of Applied Physics, 2006, 99, 034105.	1.1	46
260	InMnO3: A biferroic. Journal of Applied Physics, 2006, 100, 076104.	1.1	28
261	Dielectric properties of c-axis oriented Zn1â^'xMgxO thin films grown by multimagnetron sputtering. Applied Physics Letters, 2006, 89, 082905.	1.5	46
262	EFFECT OF MANGANESE DOPING ON THE ELECTRICAL CHARACTERISTICS OF SOL-GEL DERIVED LEAD ZIRCONATE TITANATE THIN FILMS. Integrated Ferroelectrics, 2006, 82, 65-80.	0.3	3
263	AC properties of laser ablated La-modified lead titanate thin films. Thin Solid Films, 2005, 474, 1-9.	0.8	43
264	Enhanced ferroelectric properties of vanadium doped bismuth titanate (BTV) thin films grown by pulsed laser ablation technique. Solid State Communications, 2005, 133, 611-614.	0.9	15
265	Deep level transient spectroscopy studies on BaTiO3and Ba1–xCaxTiO3thin films deposited on Si substrates. Semiconductor Science and Technology, 2005, 20, 250-255.	1.0	5
266	dc leakage behavior in vanadium-doped bismuth titanate thin films. Journal of Applied Physics, 2005, 98, 094112.	1.1	38
267	Dielectric phase-transition and polarization studies in stepped and compositionally graded lead magnesium niobate–lead titanate relaxor thin films. Journal of Applied Physics, 2005, 98, 014105.	1.1	10
268	High Energy Oxygen Ion Induced Modifications in Ferroelectric SrBi2Ta2O9Thin Films. Ferroelectrics, 2005, 328, 103-109.	0.3	3
269	Enhanced tunability and phase transition studies in compositionally varying lead magnesium niobate–lead titanate multilayered thin films. Applied Physics Letters, 2005, 86, 092902.	1.5	13

BiferroicYCrO3. Physical Review B, 2005, 72, .

1.1 209

#	Article	IF	CITATIONS
271	Impact of microstructure on electrical characteristics of laser ablation grown ZrTiO4thin films on Si substrate. Journal Physics D: Applied Physics, 2005, 38, 41-50.	1.3	20
272	Investigation of Relaxor Behavior in Pb(Mgg1/3Nb2/3)O3-PbTiO3Thin Films. Ferroelectrics, 2004, 306, 17-27.	0.3	1
273	Impact of microstructure on dielectric properties of Pb(Mg1/3Nb2/3)O3–PbTiO3 thin films. Materials Science and Engineering B: Solid-State Materials for Advanced Technology, 2004, 106, 111-119.	1.7	12
274	Effect of electric field on dielectric response of PMN–PT thin films. , 2004, 113, 190-190.		5
275	Dielectric relaxation in laser ablated polycrystalline ZrTiO[sub 4] thin films. Journal of Applied Physics, 2003, 94, 5135.	1.1	60
276	Relaxor type perovskites: Primary candidates of nano-polar regions. Journal of Chemical Sciences, 2003, 115, 775-788.	0.7	10
277	Study of La-modified antiferroelectric PbZrO3 thin films. Thin Solid Films, 2003, 423, 88-96.	0.8	21
278	High energy Li ion irradiation effects in ferroelectric PZT and SBT thin films. Thin Solid Films, 2003, 434, 40-48.	0.8	21
279	Structural and optical properties of CuIn1â^'xAlxSe2 thin films prepared by four-source elemental evaporation. Solid State Communications, 2003, 127, 243-246.	0.9	24
280	Study of relaxor-like behaviour of laser ablated (Pb, La)Tio3 thin films. Solid State Communications, 2003, 127, 247-251.	0.9	8
281	Dielectric response and impedance spectroscopy of 0.7Pb(Mg1/3Nb2/3)O3–0.3PbTiO3 thin films. Materials Science and Engineering B: Solid-State Materials for Advanced Technology, 2003, 98, 204-212.	1.7	34
282	Ac conductivity studies on the Li irradiated PZT and SBT ferroelectric thin films. Materials Science and Engineering B: Solid-State Materials for Advanced Technology, 2003, 100, 93-101.	1.7	30
283	Role of La0.5Sr0.5CoO3 template layers on dielectric and electrical properties of pulsed-laser ablated Pb(Nb2/3Mg1/3)O3–PbTiO3 thin films. Thin Solid Films, 2003, 424, 274-282.	0.8	30
284	Normal ferroelectric to relaxor behavior in laser ablated Ca-doped barium titanate thin films. Journal of Applied Physics, 2003, 94, 7702.	1.1	95
285	Growth and electrical characterization of laser ablated highly oriented zirconium titanate thin films in a metalÂoxide semiconductor configuration. Semiconductor Science and Technology, 2003, 18, 183-189.	1.0	14
286	Interface states of laser ablated BaTiO3 and Ba0.9Ca0.1TiO3 thin films in MFS structure determined by DLTS and C – V technique. Materials Research Society Symposia Proceedings, 2003, 784, 3111.	0.1	0
287	Growth and Studies of Calcium Doped Laser Ablated Barium Titanate Thin Films. Integrated Ferroelectrics, 2003, 54, 747-754.	0.3	0
288	Effect of AC&DC Field on the Dielectric Response of (Pb,La)TiO 3 Thin Films. Integrated Ferroelectrics, 2003, 54, 665-677.	0.3	0

#	Article	IF	CITATIONS
289	Electrical properties of ferroelectric YMnO3films deposited on n-type Si(111) substrates. Journal Physics D: Applied Physics, 2003, 36, 2134-2140.	1.3	14
290	Analysis of leakage current conduction phenomenon in thin SrBi2Ta2O9 films grown by excimer laser ablation. Journal of Applied Physics, 2002, 91, 4543-4548.	1.1	31
291	Impact of Sr content on dielectric and electrical properties of pulsed laser ablated SrBi2Ta2O9 thin films. Journal of Applied Physics, 2002, 92, 1056-1061.	1.1	7
292	ac transport studies of La-modified antiferroelectric lead zirconate thin films. Physical Review B, 2002, 65, .	1.1	30
293	Leakage current conduction of pulsed excimer laser ablated BaBi2Nb2O9 thin films. Journal of Applied Physics, 2002, 92, 415-420.	1.1	25
294	Alternating Current Conduction and Impedance Spectroscopy Analysis on Pulsed Excimer Laser Ablated (Pb, La)TiO 3 Thin Films. Integrated Ferroelectrics, 2002, 46, 143-152.	0.3	2
295	The Thickness Dependence of the Electrical and Dielectric Properties in the Laser Ablated SrBi 2 Nb 2 O 9 Thin Films. Integrated Ferroelectrics, 2002, 50, 159-169.	0.3	1
296	Dielectric Properties of Pulsed Excimer Laser Ablated BaBi2Nb2O9 Thin Films. Materials Research Society Symposia Proceedings, 2002, 748, 1.	0.1	0
297	MFIS and MFS structures using SrBi2Ta2O9 thin films for the FRAM applications. Materials Research Society Symposia Proceedings, 2002, 747, 1.	0.1	0
298	MFIS and MFS structures using SrBi2Ta2O9 thin films for the FRAM applications. Materials Research Society Symposia Proceedings, 2002, 748, 1.	0.1	0
299	Study of Relaxor Behavior of 0.7Pb(Mg 1/3 Nb 2/3)O 3 -0.3PbTiO 3 Thin Films. Integrated Ferroelectrics, 2002, 46, 153-162.	0.3	1
300	Study of Thickness Dependence on Electrical Properties of (Pb,La)TiO 3 Thin Films for Memory Applications. Integrated Ferroelectrics, 2002, 46, 133-141.	0.3	1
301	Dielectric properties of La-modified antiferroelectric PbZrO3 thin films. Materials Science and Engineering B: Solid-State Materials for Advanced Technology, 2002, 88, 22-25.	1.7	16
302	Reversible and irreversible switching processes in pure and lanthanum modified lead zirconate thin films. Materials Science and Engineering B: Solid-State Materials for Advanced Technology, 2002, 94, 218-222.	1.7	7
303	Electrical characterization of Ba(Zr0.1Ti0.9)O3 thin films grown by pulsed laser ablation technique. Materials Science and Engineering B: Solid-State Materials for Advanced Technology, 2002, 95, 124-130.	1.7	16
304	Investigation of reversible and irreversible polarizations in thin films of SrBi2(Ta0.5,Nb0.5)2O9. Thin Solid Films, 2002, 422, 155-160.	0.8	16
305	Pulsed excimer laser ablation growth and characterization of Ba(Sn0.1Ti0.9)O3 thin films. Solid State Communications, 2002, 121, 329-332.	0.9	23
306	Growth and characterization of Ba(Zr0.1Ti0.9)O3 thin films deposited by pulsed excimer laser ablation. Solid State Communications, 2002, 122, 429-432.	0.9	8

#	Article	IF	CITATIONS
307	Dielectric and ferroelectric response of sol–gel derived Pb0.85La0.15TiO3 ferroelectric thin films on different bottom electrodes. Thin Solid Films, 2002, 406, 30-39.	0.8	12
308	Backward switching phenomenon from field forced ferroelectric to antiferroelectric phases in antiferroelectric PbZrO3 thin films. Journal of Applied Physics, 2001, 89, 4541-4547.	1.1	56
309	Effect of neodymium (Nd) doping on the dielectric and ferroelectric characteristics of sol-gel derived lead zirconate titanate (53/47) thin films. Journal of Applied Physics, 2001, 90, 2975-2984.	1.1	69
310	Analysis of Alternating Current Conduction and Impedance Spectroscopy Study of BaBi2Nb2O9 Thin Films. Materials Research Society Symposia Proceedings, 2001, 688, 1.	0.1	0
311	Impact of Template Layers on Dielectric and Electrical Properties of Pulsed-Laser Ablated Pb(Mg1/3) Tj ETQq1 1 C	.784314 r 0.1	gBT /Overloc
312	Study of layered structured ferroelectric materials grown by laser ablation. Ferroelectrics, 2001, 260, 161-167.	0.3	0
313	Antiferroelectric thin films for MEMs applications. Ferroelectrics, 2001, 263, 39-44.	0.3	14
314	Dielectric response and complex impedance spectroscopy studies in pulsed laser ablated (Ba, Sr)TiO3 thin films. Integrated Ferroelectrics, 2001, 33, 331-342.	0.3	5
315	Laser ablation and characterization of cabi2ta2o9 thin films. Integrated Ferroelectrics, 2001, 36, 63-71.	0.3	1
316	Study of pulsed laser deposited lead lanthanum titanate thin films. Thin Solid Films, 2001, 389, 84-90.	0.8	13
317	Study of AC electrical properties in multigrain antiferroelectric lead zirconate thin films. Thin Solid Films, 2001, 391, 126-132.	0.8	16
318	Study of pulsed laser ablated CaBi2Ta2O9 thin films. Solid State Communications, 2001, 119, 127-131.	0.9	5
319	Temperature dependence on the response of inversion layer with zirconium titanate as oxide in MOS configuration. Solid State Communications, 2001, 120, 379-382.	0.9	11
320	Electrical transport characteristics of Au/n-GaAs Schottky diodes on n-Ge at low temperatures. Solid-State Electronics, 2001, 45, 133-141.	0.8	160
321	Doping dependence of the barrier height and ideality factor of Au/n-GaAs Schottky diodes at low temperatures. Physica B: Condensed Matter, 2001, 307, 125-137.	1.3	114
322	Electrical properties of La-graded heterostructure of Pb1â^'xLaxTiO3 thin films. Materials Science and Engineering B: Solid-State Materials for Advanced Technology, 2001, 86, 172-177.	1.7	9
323	Interface states density distribution in Au/n-GaAs Schottky diodes on n-Ge and n-GaAs substrates. Materials Science and Engineering B: Solid-State Materials for Advanced Technology, 2001, 87, 141-147.	1.7	89
324	AC and DC conductivity studies in pulsed laser ablated (Ba, Sr)TiO3 thin films. Integrated Ferroelectrics, 2001, 33, 353-361.	0.3	3

#	Article	IF	CITATIONS
325	Antiferroelectric lead zirconate thin films by excimer laser ablation. Integrated Ferroelectrics, 2001, 35, 249-259.	0.3	0
326	Ferroelectric thin films: Preparation and characterization. Thin Films, 2001, , 375-434.	0.2	1
327	Effect of acceptor and donor dopants on polarization components of lead zirconate titanate thin films. Applied Physics Letters, 2001, 79, 239-241.	1.5	39
328	Large reduction of leakage current by graded-layer La doping in (Ba0.5, Sr0.5)TiO3 thin films. Applied Physics Letters, 2001, 79, 111-113.	1.5	35
329	Transient analysis in Al-doped barium strontium titanate thin films grown by pulsed laser deposition. Journal of Applied Physics, 2001, 90, 1250-1254.	1.1	14
330	Self-annihilation of antiphase boundaries in GaAs epilayers on Ge substrates grown by metal-organic vapor-phase epitaxy. Journal of Applied Physics, 2001, 89, 5972-5979.	1.1	39
331	Improvement of the degradation characteristics of sol-gel derived PZT (53/47) thin films : Effect of conventional and graded iron doping. Integrated Ferroelectrics, 2001, 39, 127-136.	0.3	8
332	CaBi2Ta2O9 ferroelectric thin films prepared by pulsed laser deposition. Applied Physics Letters, 2001, 78, 2925-2927.	1.5	16
333	AC electrical property studies on SrBi2(Ta0.5,Nb0.5)2O9 thin films by excimer laser ablation. Integrated Ferroelectrics, 2001, 32, 101-119.	0.3	1
334	Micro-Raman and dielectric phase transition studies in antiferroelectric PbZrO3 thin films. Applied Physics Letters, 2001, 78, 1730-1732.	1.5	25
335	Structural and electrical characteristics of Pb0.90La0.15TiO3 thin films on different bottom electrodes. Journal of Applied Physics, 2001, 89, 5637-5643.	1.1	22
336	Growth and study of SrBi2 (Ta, Nb)2 O9 thin films by pulsed excimer laser ablation. Solid State Communications, 2000, 114, 585-588.	0.9	9
337	Pulsed excimer laser ablated copper indium diselenide thin films. Solid State Communications, 2000, 116, 649-653.	0.9	18
338	Effects of thin oxide in metal–semiconductor and metal–insulator–semiconductor epi-GaAs Schottky diodes. Solid-State Electronics, 2000, 44, 1089-1097.	0.8	139
339	Dielectric and dc electrical studies of antiferroelectric lead zirconate thin films. Materials Science and Engineering B: Solid-State Materials for Advanced Technology, 2000, 78, 1-10.	1.7	10
340	Dielectric relaxation in antiferroelectric multigrain PbZrO3 thin films. Materials Science and Engineering B: Solid-State Materials for Advanced Technology, 2000, 78, 75-83.	1.7	29
341	Transmission electron microscopic study of GaAs/Ge heterostructures grown by low-pressure metal organic vapor phase epitaxy. Materials Research Bulletin, 2000, 35, 125-133.	2.7	14
342	Atomic force microscopic study of surface morphology in Si-doped epi-GaAs on Ge substrates: effect of off-orientation. Materials Research Bulletin, 2000, 35, 909-919.	2.7	22

#	Article	IF	CITATIONS
343	Excimer laser ablation processed ferroelectric and antiferroelectric thin films. Integrated Ferroelectrics, 2000, 31, 1-12.	0.3	1
344	Alternating current electrical properties of antiferroelectric lead zirconate thin films by pulsed excimer laser ablation. Journal of Applied Physics, 2000, 88, 2072-2080.	1.1	18
345	Growth and characterization of excimer laser-ablated BaBi2Nb2O9 thin films. Applied Physics Letters, 2000, 77, 3818-3820.	1.5	25
346	Microstructure related influence on the electrical properties of pulsed laser ablated (Ba, Sr)TiO3 thin films. Journal of Applied Physics, 2000, 88, 3506-3513.	1.1	37
347	Alternating current conduction behavior of excimer laser ablated SrBi[sub 2]Nb[sub 2]O[sub 9] thin films. Journal of Applied Physics, 2000, 88, 4294.	1.1	50
348	Field-induced dielectric properties of laser ablated antiferroelectric (Pb0.99Nb0.02)(Zr0.57Sn0.38Ti0.05)0.98O3 thin films. Applied Physics Letters, 2000, 77, 4208-4210.	1.5	4
349	Impact of microstructure on the electrical stress induced effects of pulsed laser ablated (Ba, Sr)TiO3 thin films. Journal of Applied Physics, 2000, 87, 3056-3062.	1.1	31
350	Dielectric response in pulsed laser ablated (Ba,Sr)TiO3 thin films. Journal of Applied Physics, 2000, 87, 849-854.	1.1	71
351	Growth and characterization of SrBi2Nb2O9 thin films by pulsed-laser ablation. Applied Physics Letters, 1999, 75, 2656-2658.	1.5	31
352	Breakdown characteristics of MOVPE grown Si-doped GaAs Schottky diodes. Solid-State Electronics, 1999, 43, 2135-2139.	0.8	5
353	Study of the electrical properties of pulsed laser ablated (Ba0.5Sr0.5)TiO3 thin films. Materials Science and Engineering B: Solid-State Materials for Advanced Technology, 1999, 57, 135-146.	1.7	47
354	Si incorporation and Burstein–Moss shift in n-type GaAs. Materials Science and Engineering B: Solid-State Materials for Advanced Technology, 1999, 60, 1-11.	1.7	39
355	Impedance-fatigue correlated studies on SrBi2Ta2O9. Materials Science and Engineering B: Solid-State Materials for Advanced Technology, 1999, 64, 149-156.	1.7	35
356	Antiferroelectric lead zirconate thin films by pulsed laser ablation. Materials Science and Engineering B: Solid-State Materials for Advanced Technology, 1999, 64, 54-59.	1.7	13
357	Anomalous current transport in Au/low-doped n-GaAs Schottky barrier diodes at low temperatures. Applied Physics A: Materials Science and Processing, 1999, 68, 49-55.	1.1	74
358	Growth, optical, and electron transport studies across isotype n-GaAs/n-Ge heterojunctions. Journal of Vacuum Science & Technology an Official Journal of the American Vacuum Society B, Microelectronics Processing and Phenomena, 1999, 17, 1003.	1.6	16
359	Growth and study of antiferroelectric lead zirconate thin films by pulsed laser ablation. Journal of Applied Physics, 1999, 86, 5862-5869.	1.1	76
360	OMVPE growth of undoped and Si-doped GaAs epitaxial layers on Ge. Journal of Crystal Growth, 1998, 193, 501-509.	0.7	14

#	Article	IF	CITATIONS
361	Correlation of compensation in Si-doped GaAs between electrical and optical methods. Solid State Communications, 1998, 108, 457-461.	0.9	4
362	Role of growth conditions and Bi-content on the properties of SrBi2Ta2O9 thin films. Solid State Communications, 1998, 108, 759-763.	0.9	10
363	Comparative studies of Si-doped n-type MOVPE GaAs on Ge and GaAs substrates. Materials Science and Engineering B: Solid-State Materials for Advanced Technology, 1998, 55, 53-67.	1.7	14
364	Low temperature photoluminescence properties of Zn-doped GaAs. Materials Science and Engineering B: Solid-State Materials for Advanced Technology, 1998, 57, 62-70.	1.7	18
365	Photoluminescence studies on Si-doped GaAs/Ge. Journal of Applied Physics, 1998, 83, 4454-4461.	1.1	27
366	Zn incorporation and band gap shrinkage in p-type GaAs. Journal of Applied Physics, 1997, 82, 4931-4937.	1.1	34
367	Electron cyclotron resonance plasma assisted sputter deposition of boron nitride films. Applied Physics Letters, 1997, 70, 628-630.	1.5	11
368	Studies on structural and electrical properties of barium strontium titanate thin films developed by metallo-organic decomposition. Thin Solid Films, 1997, 305, 144-156.	0.8	66
369	Effect of ratio on the optical properties of MOCVD grown undoped GaAs layers. Solid State Communications, 1997, 103, 411-416.	0.9	6
370	Growth and Characterization of GaAs Epitaxial Layers by MOCVD. Materials Research Society Symposia Proceedings, 1996, 421, 281.	0.1	3
371	Sputter Synthesis of Ferroelectric Films and Heterostructures. MRS Bulletin, 1996, 21, 25-30.	1.7	37
372	Rapid thermal processed thin films of niobium pentoxide (Nb 2 O 5) deposited by reactive magnetron sputtering. Thin Solid Films, 1995, 261, 18-24.	0.8	7
373	Rapid thermal processed thin films of reactively sputtered Ta2O5. Thin Solid Films, 1995, 258, 230-235.	0.8	95
374	Reactive magnetron coâ€sputtered antiferroelectric lead zirconate thin films. Applied Physics Letters, 1995, 67, 2014-2016.	1.5	92
375	Structures and electrical properties of barium strontium titanate thin films grown by multi-ion-beam reactive sputtering technique. Journal of Materials Research, 1995, 10, 708-726.	1.2	99
376	Pt/Ti/SiO ₂ /Si substrates. Journal of Materials Research, 1995, 10, 1508-1515.	1.2	90
377	Thicknessâ€dependent electrical characteristics of lead zirconate titanate thin films. Journal of Applied Physics, 1995, 77, 3981-3986.	1.1	126
378	Low Energy Ion Bombardment Induced Effects in Multicomponent Electroceramic Thin Films. , 1995, , 23-51.		2

#	Article	IF	CITATIONS
379	Dependence of perovskite/pyrochlore phase formation on oxygen stoichiometry in PLT thin films. Journal of Materials Research, 1994, 9, 699-711.	1.2	48
380	Study of electrical properties of pulsed excimer laser deposited strontium titanate films. Journal of Applied Physics, 1994, 75, 2604-2611.	1.1	36
381	Pulsed excimer laser ablation of (Pb,La)TiO3thin films for dynamic random access memory devices. Applied Physics Letters, 1994, 64, 1591-1593.	1.5	35
382	Pulsed laser deposition of strontium titanate thin films for dynamic random access memory applications. Thin Solid Films, 1994, 249, 100-108.	0.8	8
383	Current-voltage characteristics of ultrafine-grained ferroelectric Pb(Zr, Ti)O ₃ thin films. Journal of Materials Research, 1994, 9, 1484-1498.	1.2	154
384	Spectroscopic ellipsometry studies on ion beam sputter deposited Pb(Zr, Ti)O3 films on sapphire and Pt-coated silicon substrates. Thin Solid Films, 1993, 230, 15-27.	0.8	47
385	Effect of heating rate on the crystallization behavior of amorphous PZT thin films. Thin Solid Films, 1993, 223, 327-333.	0.8	82
386	Origin of Orientation in Sol-Gel-Derived Lead Titanate Films. Journal of the American Ceramic Society, 1993, 76, 1345-1348.	1.9	65
387	Processâ€property correlations of excimer laser ablated bismuth titanate films on silicon. Journal of Applied Physics, 1993, 74, 7551-7560.	1.1	15
388	Structural and electrical characteristics of SrTiO3 thin films for dynamic random access memory applications. Journal of Applied Physics, 1993, 73, 7627-7634.	1.1	195
389	Electrical properties of strontium titanate thin films by multiâ€ionâ€beam reactive sputtering technique. Applied Physics Letters, 1993, 63, 1038-1040.	1.5	34
390	Composition/structure/property relations of multi-ion-beam reactive sputtered lead lanthanum titanate thin films: Part III. Electrical properties. Journal of Materials Research, 1993, 8, 2203-2215.	1.2	20
391	Lowâ€energy oxygen ion bombardment effect on BaTiO3thin films grown by multiâ€ionâ€beam reactive sputtering technique. Applied Physics Letters, 1993, 63, 734-736.	1.5	7
392	Switching, fatigue, and retention in ferroelectric Bi4Ti3O12thin films. Applied Physics Letters, 1993, 62, 1928-1930.	1.5	146
393	Electronâ€cyclotronâ€resonance plasmaâ€assisted radioâ€frequencyâ€sputtered strontium titanate thin films. Journal of Applied Physics, 1993, 74, 6851-6858.	1.1	22
394	Nonlinear electrical properties of leadâ€lanthanumâ€titanate thin films deposited by multiâ€ionâ€beam reactive sputtering. Journal of Applied Physics, 1993, 74, 1949-1959.	1.1	69
395	Enhanced electrical properties of ferroelectric Pb(Zr0.5, Ti0.5)O3thin films grown with lowâ€energy oxygen ion assistance. Journal of Applied Physics, 1993, 74, 3373-3382.	1.1	36
396	Switching characteristics of multiâ€ionâ€beam reactive sputter deposited Pb(Zr,Ti)O3thin films. Applied Physics Letters, 1993, 62, 651-653.	1.5	5

#	Article	IF	CITATIONS
397	Excimer laser ablated barium strontium titanate thin films for dynamic random access memory applications. Applied Physics Letters, 1993, 62, 1056-1058.	1.5	149
398	Composition/structure/property relations of multi-ion-beam reactive sputtered lead lanthanum titanate thin films: Part II. Textured microstructure development. Journal of Materials Research, 1993, 8, 2191-2202.	1.2	13
399	Ferroelectric Thin Films and Device Applications. , 1993, , 601-625.		2
400	Electrical characteristics of excimer laser ablated bismuth titanate films on silicon. Journal of Applied Physics, 1992, 72, 3617-3621.	1.1	59
401	Pulsed excimer laser deposition of ferroelectric thin films. Integrated Ferroelectrics, 1992, 1, 253-268.	0.3	13
402	Excimer laser ablated strontium titanate thin films for dynamic random access memory applications. Applied Physics Letters, 1992, 60, 2478-2480.	1.5	53
403	Effect of low pressure dc plasma discharge on laser ablated ferroelectric Pb(Zr,Ti)O3thin films. Journal of Applied Physics, 1992, 72, 620-625.	1.1	14
404	Strontium titanate thin films by rapid thermal processing. Applied Physics Letters, 1992, 61, 1525-1527.	1.5	49
405	Growth of ferroelectric oxide thin films by excimer laser ablation. Journal of Vacuum Science and Technology A: Vacuum, Surfaces and Films, 1992, 10, 1815-1820.	0.9	12
406	Pulsed excimer laser ablated barium titanate thin films. Applied Physics Letters, 1992, 61, 2057-2059.	1.5	89
407	Property modification of ferroelectric Pb(Zr,Ti)O3thin films by lowâ€energy oxygen ion bombardment during film growth. Applied Physics Letters, 1992, 61, 1246-1248.	1.5	28
408	Rapid thermally processed ferroelectric Bi4Ti3O12thin films. Journal of Applied Physics, 1992, 72, 5517-5519.	1.1	76
409	Polarization reversal and high dielectric permittivity in lead magnesium niobate titanate thin films. Applied Physics Letters, 1992, 60, 1187-1189.	1.5	56
410	Multiâ€ionâ€beam reactive sputter deposition of ferroelectric Pb(Zr,Ti)O3thin films. Journal of Applied Physics, 1992, 71, 376-388.	1.1	128
411	Oriented lead germanate thin films by excimer laser ablation. Applied Physics Letters, 1992, 60, 827-829.	1.5	14
412	Recent advances in physical vapor growth processes for ferroelectric thin films. Journal of Vacuum Science and Technology A: Vacuum, Surfaces and Films, 1992, 10, 1569-1577.	0.9	27
413	Recent advances in the deposition of ferroelectric thin films. Integrated Ferroelectrics, 1992, 1, 161-180.	0.3	9
414	Composition/structure/property relations of multi-ion-beam reactive sputtered lead lanthanum titanate thin films: Part I. Composition and structure analysis. Journal of Materials Research, 1992, 7, 3039-3055.	1.2	43

#	Article	IF	CITATIONS
415	Pulsed excimer laser deposition and characterization of ferroelectric Pb(Zr _{0.52} Ti _{0.48})O ₃ thin films. Journal of Materials Research, 1992, 7, 2521-2529.	1.2	32
416	Development of ferroelectric Pb(ZrxTi1â^'x)O3 thin films by metallo-organic decomposition process and rapid thermal annealing. Integrated Ferroelectrics, 1992, 1, 111-127.	0.3	33
417	Excimer laserâ€ablated bismuth titanate thin films. Applied Physics Letters, 1992, 60, 781-783.	1.5	46
418	Structural and electrical studies on rapid thermally processed ferroelectric Bi4Ti3O12thin films by metalloâ€organic solution deposition. Journal of Applied Physics, 1992, 72, 5827-5833.	1.1	113
419	Excimer laser ablation of ferroelectric Pb(Zr,Ti)O3 thin films with low pressure directâ€current glow discharge. Journal of Vacuum Science and Technology A: Vacuum, Surfaces and Films, 1992, 10, 1827-1831.	0.9	21
420	Excimer laser ablated deposition of ferroelectric lead germanate thin films. Thin Solid Films, 1992, 219, 162-169.	0.8	6
421	Excimer laser ablated lead zirconate titanate thin films. Journal of Applied Physics, 1991, 69, 7930-7932.	1.1	75
422	Studies of MZS and MZOS Structures with Zinc Oxide Deposited by Conventional Rf Diode and Magnetron Sputtering Techniques. Materials Research Society Symposia Proceedings, 1986, 77, 289.	0.1	1
423	Rf Magnetron Sputter Deposition and Characterization of Aluminum Nitride thin Films. Materials Research Society Symposia Proceedings, 1986, 77, 399.	0.1	4
424	Position and pressure effects in rf magnetron reactive sputter deposition of piezoelectric zinc oxide. Journal of Applied Physics, 1984, 56, 3308-3318.	1.1	111
425	Radio frequency magnetron sputtering of multicomponent ferroelectric oxides. Journal of Vacuum Science and Technology A: Vacuum, Surfaces and Films, 1984, 2, 303-306.	0.9	12
426	Electrical characterization of amorphous germanium dioxide films. Thin Solid Films, 1984, 113, 173-184.	0.8	10
427	I-V & C-V characteristics of ferroelectric lead germanate on silicon. Ferroelectrics, 1983, 50, 117-122.	0.3	6
428	rf planar magnetron sputtering and characterization of ferroelectric Pb(Zr,Ti)O3films. Journal of Applied Physics, 1983, 54, 6601-6609.	1.1	214
429	lâ€VandCâ€Vstudies of evaporated amorphous arsenic telluride film on crystalline silicon. Journal of Applied Physics, 1983, 54, 1383-1389.	1.1	5
430	R.F. magnetron sputtering of ferroelectric PZT films. Ferroelectrics, 1983, 51, 93-98.	0.3	6
431	Ferroelectric field effect in Te on TGSe substrate. Solid-State Electronics, 1981, 24, 91-95.	0.8	1
432	A study of the ferroelectric field effect in Te films on lead germanate, triglycine sulphate, and triglycine selenate substrates. Journal of Applied Physics, 1981, 52, 5274-5282.	1.1	6

#	Article	IF	CITATIONS
433	Electrical switching in single crystal VO2. Solid-State Electronics, 1980, 23, 649-654.	0.8	19
434	Preparation and properties of thermally evaporated lead germanate films. Journal of Applied Physics, 1980, 51, 5408.	1.1	30
435	Low frequency electrical behavior of ferroelectric MASD. Journal of Chemical Physics, 1978, 69, 3039-3043.	1.2	3
436	Impact of microstructure on the electrical properties of zirconium titanate thin films in MOS configuration. , 0, , .		1
437	Group III-Nitrides and Their Hybrid Structures for Next-Generation Photodetectors. , 0, , .		2
438	Pulsed Laser Deposition of Transition Metal Dichalcogenides-Based Heterostructures for Efficient Photodetection. , 0, , .		2
439	Dependence of defect structure on In concentration in InGaN epilayers grown on AlN/Si (111) substrate. Materials Advances, 0, , .	2.6	0